

Intensive systolic blood pressure treatment remodels brain perivascular spaces: A secondary analysis of the Systolic Pressure Intervention Trial (SPRINT)

Kyle C. Kern^{a,*}, Ilya M. Nasrallah^b, Robert Nick Bryan^b, David M. Reboussin^c, Clinton B. Wright^d

^a Intramural Stroke Branch, National Institute of Neurological Disorders and Stroke, National Institutes of Health, Bethesda, MD, USA

^b Department of Radiology, University of Pennsylvania, Philadelphia, PA, USA

^c Biostatistics and Data Science, Wake Forest University, Wake Forest, NC, USA

^d Division of Clinical Research, National Institute of Neurological Disorders and Stroke, National Institutes of Health, Bethesda, MD, USA

ABSTRACT

Background: Brain perivascular spaces (PVS) are part of the glymphatic system and facilitate clearance of metabolic byproducts. Since enlarged PVS are associated with vascular health, we tested whether intensive systolic blood pressure (SBP) treatment affects PVS structure.

Methods: This is a secondary analysis of the Systolic Pressure Intervention Trial (SPRINT) MRI Substudy: a randomized trial of intensive SBP treatment to goal < 120 mm Hg vs < 140 mm Hg. Participants had increased cardiovascular risk, pre-treatment SBP 130–180, and no clinical stroke, dementia, or diabetes. Brain MRIs acquired at baseline and follow-up were used to automatically segment PVS in the supratentorial white matter and basal ganglia using a Frangi filtering method. PVS volumes were quantified as a fraction of the total tissue volume. The effects of SBP treatment group and major antihypertensive classes on PVS volume fraction were separately tested using linear mixed-effects models while covarying for MRI site, age, sex, Black race, baseline SBP, history of cardiovascular disease (CVD), chronic kidney disease, and white matter hyperintensities (WMH).

Results: For 610 participants with sufficient quality MRI at baseline (mean age 67 ± 8 , 40 % female, 32 % Black), greater PVS volume fraction was associated with older age, male sex, non-Black race, concurrent CVD, WMH, and brain atrophy. For 381 participants with MRI at baseline and at follow-up (median \pm IQR = 3.9 ± 0.4 years), intensive treatment was associated with decreased PVS volume fraction relative to standard treatment (interaction coefficient: -0.029 [-0.055 to -0.0029] $p = 0.029$). Reduced PVS volume fraction was also associated with exposure to calcium channel blockers (CCB).

Conclusions: PVS enlargement was partially reversed in the intensive SBP treatment group. The association with CCB use suggests that improved vascular compliance may be partly responsible. Improved vascular health may facilitate glymphatic clearance.

[Clinicaltrials.gov](https://clinicaltrials.gov): NCT01206062.

1. Introduction

Brain perivascular spaces (PVS) visible on routine MRI are an emerging biomarker for cerebral small vessel disease (CSVD). Enlargement of PVS is thought to reflect stagnant flow, and is associated with aging, hypertension, and other cerebrovascular risk factors (Rouhl et al., 2008; Zhu et al., 2010; Huijts et al., 2014). PVS are part of the glymphatic system, which facilitates the exchange and clearance of solutes between the cerebrospinal fluid and interstitial fluid (Wardlaw et al., 2020). Based on preclinical models, fluid movement in the PVS is thought to be partly driven by arterial pulsations and low frequency vasomotor oscillations (Wardlaw et al., 2020; Rennels et al., 1985; Mestre et al., 2018; van Veluw et al., 2020). Thus, arterial stiffening

associated with arteriosclerosis and aging potentially impairs bulk flow, leading to PVS enlargement and impaired glymphatic clearance (Mestre et al., 2018; van Veluw et al., 2020). Since glymphatic circulation is thought to facilitate clearance of protein aggregates including amyloid (Iliff et al., 2012), enlarged PVS may reflect a process by which poor vascular health contributes to neurodegenerative disease (Wardlaw et al., 2020).

Most prior studies have relied on visual rating scales to quantify PVS (Potter et al., 2015), but volumetric quantification may be more sensitive to longitudinal changes. Established methods permit unbiased calculation of PVS volumes (Ballerini et al., 2018; Sepehrband et al., 2019) that have revealed the dynamic nature of PVS in development (Lynch et al., 2022), cognitive impairment (Sepehrband et al., 2021),

* Corresponding author at: 10 Center Drive, 4D37, Bethesda, MD 20892, USA.
E-mail address: kyleckern@yahoo.com (K.C. Kern).

<https://doi.org/10.1016/j.nicl.2023.103513>

Received 25 July 2023; Received in revised form 9 September 2023; Accepted 20 September 2023

Available online 23 September 2023

2213-1582/Published by Elsevier Inc. This is an open access article under the CC BY license (<http://creativecommons.org/licenses/by/4.0/>).

Parkinson's disease (Donahue et al., 2021), and space flight (Barisano et al., 2022).

While enlarged PVS are associated with hypertension (Zhu et al., 2010), whether antihypertensive therapy and intensive blood pressure treatment can affect PVS structure is unknown. The SPRINT trial evaluated the effects of intensive systolic blood pressure treatment, targeting SBP less than 120 mm Hg vs the standard therapy goal of less than 140 mm Hg, on cardiovascular and cognitive outcomes and, in a subsample, brain imaging markers (Williamson et al., 2019; Nasrallah et al., 2019). In this subsample, intensive therapy resulted in slower progression of the CSVD biomarker of WMH volume. In this secondary analysis of SPRINT we evaluate the effect of intensive treatment on PVS volumes. We hypothesized that automated PVS segmentation could detect longitudinal changes in PVS volume, and that intensive treatment would slow the enlargement of PVS.

2. Methods

2.1. Data availability

Anonymized trial data are available via NHLBI's BioLINCC (biolincc.nhlbi.nih.gov). Additional data supporting the findings of this study are available from the corresponding author upon reasonable request.

2.2. Trial design

The trial design, methods, primary outcomes, and protocol have been published previously (Nasrallah et al., 2019; SPRINT Research Group et al., 2015; Williamson et al., 2019). The trial and MRI substudy were approved by the institutional review board at each participating site, and each participant provided written informed consent.

2.3. Participants

Participants were recruited to the Systolic Pressure Intervention Trial (SPRINT) from clinic settings or from the community. Participants were ≥ 50 years old with SBP between 130 and 180 mm Hg at screening and had increased cardiovascular risk. Increased cardiovascular risks included clinical or subclinical cardiovascular disease (CVD), chronic kidney disease (CKD), a Framingham risk score of $\geq 15\%$, or age ≥ 75 years. Participants were excluded if they had diabetes, a history of stroke, a diagnosis of dementia or were treated with dementia medications, or lived in a nursing home. Race and ethnicity were collected via self-report per NIH guidelines. Participants were randomized by the data coordinating center, stratified by clinic site, in a 1:1 ratio to either an SBP goal < 120 mm Hg (intensive treatment; $n = 4678$) or an SBP goal < 140 mm Hg (standard treatment; $n = 4683$). The algorithms and formulary for antihypertensive treatment are published (SPRINT Research Group et al., 2015), and included all major classes, provided at no cost to participants. The protocol encouraged but did not mandate thiazide diuretics as first-line, loop diuretics for participants with CKD, and Beta-adrenergic blockers for participants with coronary artery disease.

2.4. Antihypertensive classes

Antihypertensive medications were recorded at each study visit and exposure to each class was calculated as the fraction of days taking the antihypertensive from randomization to follow-up MRI. To test the effects of antihypertensive classes on PVS volumes, some classes were combined: ACE inhibitors and angiotensin receptor blockers (ACEi/ARB), selective and non-selective beta blockers, dihydropyridine and non-dihydropyridine calcium channel blockers, and diuretics including thiazide, loop, and potassium-sparing.

2.5. Achieved systolic blood pressure

All blood pressure measures from randomization to follow-up MRI were used to calculate the achieved SBP, defined as the area under the SBP curve divided by the number of days.

2.6. MRI acquisition

All SPRINT participants accessible to one of 7 designated MRI sites were screened for the MRI substudy, a research MRI protocol designed to evaluate the primary imaging outcomes of change in cerebral white matter hyperintensity (WMH) and total brain volumes (TBV) (Nasrallah et al., 2019). Exclusion criteria for the MRI substudy included contraindications to MRI such as implanted or foreign metallic or ferromagnetic material, or severe claustrophobia. Multimodal brain MRI was obtained at baseline and planned at 48 months post-randomization. For each participant, both scans were performed on the same scanner. Due to early termination of the study due to improved cardiovascular outcomes with intensive treatment, follow up MRIs were obtained earlier than planned. All 7 sites used 3 T scanners (3 Phillips and 4 Siemens). The MRI sequence parameters remained the same throughout the study, and the protocol included 1 mm isotropic 3D T1, T2 and FLAIR sequences (Supplemental Methods). Scanner performance, monitored quarterly using phantom acquisition measurements, remained stable throughout the trial. Enrollment continued from November 8, 2010 to March 2013, with the last MRI occurring in July 2016. Of 1267 individuals screened, 793 were eligible, 670 underwent baseline MRI, and 662 had baseline T1 and T2 that passed initial quality control.

2.7. MRI processing

Image parameters were calculated as previously described, including WMH volume, TBV, total white matter (WM) volume, total gray matter (GM) volume, and total intracranial volume (TICV) (Nasrallah et al., 2019). WMH volumes were adjusted for TICV and log transformed due to skewed distribution ($\log \text{WMH} = \log(1 + \text{WMHvol}/\text{TICV})$). Brain parenchymal fraction (BPF), a marker of atrophy, was calculated as $\text{BPF} = (\text{WM} + \text{GM}) / \text{TICV}$.

2.8. Calculation of perivascular space volumes

PVS volumes were calculated using T1, T2 and FLAIR MRI following methods described by Sepehrband et al. (2019,2021) using FreeSurfer (surfer.nmr.mgh.harvard.edu/fswiki/Samseg) (Cerri et al., 2021), FSL (fsl.fmrib.ox.ac.uk/fsl) (Smith et al., 2004), and the Quantitative Imaging Toolkit (cabeen.io/qitwiki) (Cabeen et al., 2018).

T1, T2 and FLAIR images were bias-field corrected and aligned, and tissue was segmented using a multi-modality tissue segmentation algorithm to create a region-of-interest (ROI) of the supratentorial white matter and basal ganglia (Cerri et al., 2021) for PVS segmentation. The ROI mask was smoothed with a 1 mm filter while retaining edges, and a hole-filling algorithm was applied to fill regions where PVS were labelled as CSF. A ventricular mask was dilated by 1 mm to further remove the layer of voxels immediately adjacent to the ventricles from this ROI (Sepehrband et al., 2019).

T2 images were used to segment PVS within this ROI (Fig. 1). First a non-local means filter was applied to reduce Rician noise. Next a Frangi filter was applied that selects for hyperintense, tubular structures and assigns a value of "vesselness" using parameters previously established (Sepehrband et al., 2019): $\alpha = 0.5$, $\beta = 0.5$, $\gamma = 500$, $S_{\min} = 0.1$, and $S_{\max} = 5$. Next, the Frangi intensity map was scaled to the interquartile range to avoid the influence of large outliers and then thresholded using a value of 2.7, which was determined from the dataset as described below. WMH were excluded from the PVS segmentation. Individual PVS were separated using 26-point connected component analysis, and individual PVS smaller than 5 voxels were excluded to

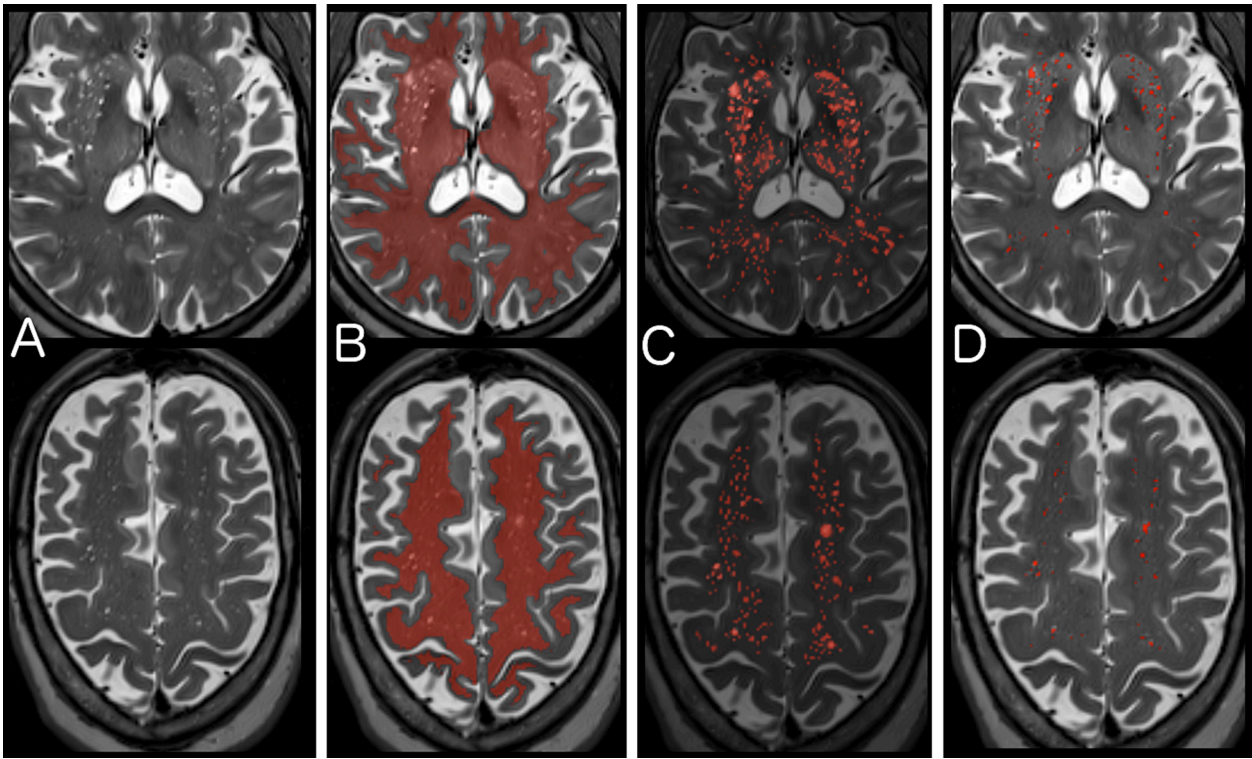


Fig. 1. Segmentation of Perivascular Spaces. A) T2 images were bias-field corrected, and then a non-local means filter was applied to reduce Rician noise. B) A region of interest (ROI) of supratentorial white matter and basal ganglia was created from the T1 and FLAIR images using Freesurfer’s SAMSEG (Cerri et al., 2021) and aligned to the T2 image. C) A Frangi filter was applied within the ROI that selects for tubular structures and assigns an intensity reflecting the “vesselness” at each voxel. D) The optimal Frangi threshold of 2.7 (standardized value) was determined empirically by comparing to visual ratings and visually confirmed for anatomical match across a random subset of 120 images.

reduce noise. Finally, the PVS volume was calculated in cm^3 and also reported as a percentage of the total ROI volume analyzed (supratentorial white matter and basal ganglia): the PVS volume fraction.

To determine the optimal Frangi threshold for T2 images in this dataset, a random sample of 120 scans were used to compare visual PVS ratings to calculated PVS volumes across a range of Frangi thresholds.

Supratentorial PVS were visually rated on T2 using an established grading system (Potter et al., 2015) for this sample by one rater and then repeated after a 2-month washout period. PVS were rated in the basal ganglia and insular region (0 to 4), and the centrum semiovale (0 to 4), providing a total supratentorial visual PVS score of 0 to 8. For these 120 scans, the Frangi image threshold was varied from 0.5 to 3.3, and a

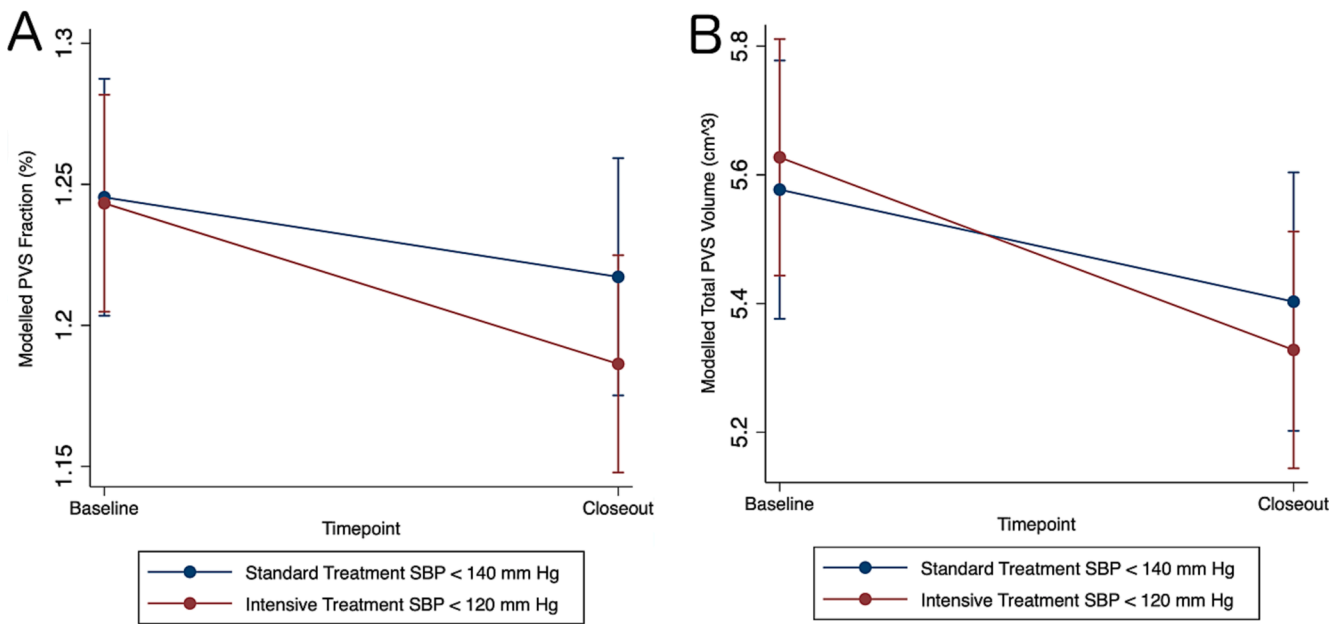


Fig. 2. Intensive Treatment Reduces PVS Volumes. A) Modelled perivascular space (PVS) volume fraction over time by systolic blood pressure (SBP) treatment group. B) Modelled total PVS volume (cm^3) over time by SBP treatment group.

correlation coefficient was calculated at each threshold between the calculated percent volume fraction and the visual rating score. The optimal threshold of 2.7 ($R = 0.510$) was determined by considering the maximal correlation coefficient and visual inspection (supplemental results; supplemental Fig. 2) (Sepehrband et al., 2019). Finally, PVS were segmented for all image sets in a fully automated fashion using a high-performance computing cluster (hpc.nih.gov), and then visually inspected (while blinded to treatment and timepoint) to ensure quality segmentation. Participants with T2 images that were of insufficient quality to visualize or segment PVS were excluded ($n = 105$ scans: 52 at baseline and 53 at follow-up). Scans were excluded primarily due to motion artifact that obscured visualization and/or PVS segmentation.

2.9. Covariates and subgroups

Covariates for all analyses included age, sex, race (Black vs not Black), CKD subgroup ($eGFR < 60$ vs ≥ 60 mL/min/1.73 m²), history of CVD, and baseline SBP. In the baseline analysis, the relationship to BPF, a marker of atrophy was tested. Since severe WMH can obscure PVS and their segmentation, logWMH was also included as a covariate. Additional covariates for change in logWMH, total brain volume (TBV), and change in TBV were added to a subsequent longitudinal model.

2.10. Statistical analysis

Predictors of baseline PVS volume fraction were determined using multiple linear regression. Mixed effects linear regression was used to estimate change in PVS volume fraction over time between treatment groups. The primary outcome of interest in model 1 was the interaction effect between treatment group and timepoint, where the interaction coefficient reflects the relative change in PVS volume fraction between treatment groups. Random effects included participant and MRI facility, while fixed effects included timepoint, treatment group, age, sex, race, CVD subgroup, CKD subgroup, baseline SBP, and logWMH. Secondly, pairwise comparisons were tested, and Bonferroni corrected, to identify within-group and between-group differences. A similar mixed effects model estimated the absolute change in total PVS volume while also adjusting for head size with TICV. Given the findings of the primary SPRINT MRI study that intensive treatment was associated with reduced WMH volume progression but also with a greater decrease in TBV (Nasrallah et al., 2019), we further tested whether PVS volume fraction changes were driven by these changes in TBV or WMH. In model 2, a confirmatory model, we used mixed effects linear regression to estimate the relative change in PVS volume fraction between treatment groups while also accounting for the mean logWMH (between-participant effect), the change in logWMH (patient-centered to reflect within-participant effect), the mean TBV (between-participant effect), and the change in TBV (patient-centered to reflect within-participant effect). Finally, to explore potential mechanisms for PVS morphological changes, we tested whether exposure to 4 major antihypertensive classes was related to change in PVS volume fraction: ACEi/ARB, beta-blockers, calcium channel blockers (CCB), or diuretics. To test this additional hypothesis in model 3, we used a mixed-effects linear model where the four interaction terms between timepoint and antihypertensive class exposure were of primary interest. The model included all four medication classes to test the individual effect of each class on change in PVS volume fraction while effectively holding the other 3 classes constant. The model also included covariates for treatment group, baseline SBP, achieved SBP, age, sex, race, CVD, CKD, logWMH, and TBV. Finally, we also reported the baseline differences between those with and without follow-up MRI (Supplemental Table 1). All hypothesis tests were 2-sided, and adjusted p-values less than 0.05 were considered statistically significant. Analyses were performed March 2022 through May 2023 using Stata v.17.0 (stata.com).

3. Results

To determine baseline predictors of PVS volume fraction, 610 participants were included (Table 1). For the longitudinal analysis, 381 participants had both baseline and follow-up MRI of sufficient quality: 207 with intensive treatment and 174 with standard treatment (Supplemental Fig. 1).

Baseline characteristics were similar between the intensive and standard SBP treatment groups (Table 1). Larger PVS volume fraction at baseline was associated with older age, male sex, non-Black race, CVD subgroup, lower logWMH, and larger BPF while controlling for MRI site (Table 2).

Over median 3.9 ± 0.4 (IQR) years to follow-up MRI (range: 3.2 to 4.8 years), mean achieved SBP was 120 ± 8 mm Hg with intensive treatment and 136 ± 7 mm Hg with standard treatment ($p < 0.001$) (Supplemental Fig. 3). At baseline, PVS volume fractions were 1.23 % in both groups while total PVS volumes were 5.45 cm³ in the intensive treatment group and 5.52 cm³ in the standard treatment group (Table 1).

In the longitudinal analysis, there was a reduction in mean PVS volume fraction in the intensive treatment group relative to the standard treatment group over time by -0.029 % (-0.055 to -0.0029 , $p = 0.029$) (Table 4, Model 1). In pairwise comparisons testing absolute group and timepoint differences, the intensive group had a -0.027 % decrease in PVS volume fraction from baseline (-0.51 to -0.0032 , $p = 0.016$) while the standard group had a non-significant decrease of -0.0017 % (-0.025 to 0.029) (Figure 2A). This equated to a -0.20 cm³ (-0.31 to -0.089 , $p < 0.001$) volume change in the intensive group and a -0.076 cm³ (-0.20 to 0.050) volume change in the standard treatment group, or a relative difference of -0.13 cm³ (-0.25 to -0.0026) for the intensive group (Figure 2B). When also accounting for changes in WMH volume and TBV previously described in this cohort, intensive treatment was associated with a relative greater decrease in PVS volume fraction

Table 1
Baseline Clinical and Imaging Measures.

	Overall	Intensive Tx	Standard Tx
N	610	324	286
% Female	40 % (245)	44 % (141)	36 % (104)
Age (years \pm SD)	68 ± 8	68 ± 8	67 ± 9
Race:			
Black	32 % (198)	31 % (102)	34 % (96)
White	66 % (403)	67 % (217)	65 % (186)
Hispanic	5 % (30)	3 % (11)	7 % (19)
Other	2 % (12)	2 % (6)	2 % (6)
Baseline SBP (mmHg)	138 ± 16	137 ± 17	137 ± 16
Framingham Score (\pm SD)	17 ± 2	17 ± 2	17 ± 2
Self-Reported History of:			
Hypertension	93 % (569)	94 % (305)	92 % (264)
Smoked > 100 lifetime cigs	53 % (324)	54 % (175)	52 % (149)
Taking Aspirin	51 % (312)	49 % (158)	54 % (154)
Cancer	13 % (80)	15 % (48)	11 % (32)
Current Smoking	12 % (77)	13 % (43)	12 % (34)
Atrial Fibrillation	7 % (40)	7 % (23)	6 % (17)
Peripheral Vascular Disease	6 % (34)	7 % (23)	4 % (11)
Heart Attack	4 % (27)	5 % (15)	4 % (12)
Prior TIA	3 % (20)	4 % (13)	2 % (7)
Congestive Heart Failure	2 % (14)	2 % (7)	2 % (7)
Seizure	1 % (7)	1 % (3)	1 % (4)
Baseline Imaging Measures:			
WMH Volume (cm ³ \pm IQR)	3.2 ± 4.6	3.1 ± 5.1	3.3 ± 4.4
Brain Parenchymal Fraction (%)	82 ± 4	82 ± 4	82 ± 4
PVS Volume (cm ³ \pm SD)	5.49 ± 1.70	5.45 ± 1.74	5.52 ± 1.67
PVS Volume Fraction (% \pm SD)	1.23 ± 0.32	1.23 ± 0.33	1.23 ± 0.31

WMH: white matter hyperintensity. PVS: perivascular space. SD: standard deviation. IQR: interquartile range.

Table 2
Baseline Predictors of PVS Volume Fraction.

Predictors:	Coefficient	95 % C.I.	Std. Beta	T-statistic	p-value
Male Sex	0.081	0.039 to 0.12	0.12	3.81	<0.001
BPF	0.012	0.0061 to 0.020	0.15	3.69	<0.001
Age	0.004	0.0085 to 0.0072	0.10	2.50	0.013
CVD Subgroup	0.067	0.0097 to 0.012	0.072	2.30	0.022
Baseline SBP	0.0025	−0.00092 to 0.0014	0.013	0.42	0.67
CKD Subgroup	−0.021	−0.065 to 0.023	−0.029	−0.93	0.35
Black Race	−0.065	−0.11 to −0.021	−0.095	−2.89	0.004
logWMH	−1.05	−1.22 to −0.89	−0.42	−12.84	<0.001

Adjusted for MRI site. BPF = Brain Parenchymal fraction. CVD = Cardiovascular Disease. SBP = Systolic Blood Pressure. CKD = Chronic Kidney Disease. WMH = White Matter Hyperintensities.

compared to standard treatment by −0.026 % [−0.052 to −0.00040, p = 0.047] (Model 2).

Finally, we tested the effects of the 4 major antihypertensive classes on mean PVS volume fraction. ACEi/ARBs were the most common class of antihypertensive at baseline, and participants were also most exposed to this class during the study. CCBs were the most frequently added medication during the study (Table 3). At baseline there were no associations between antihypertensive use and PVS volume fractions. In the longitudinal analysis, longer exposure to CCBs was associated with greater reduction in PVS volume fraction while also covarying for the other major classes, treatment group, achieved SBP, WMH volume, and TBV. Maximum CCB exposure (i.e. 100 % study duration) was associated with −0.038 % reduction in PVS volume fraction (−0.071 to −0.0048, p = 0.025) (Table 4, Model 3).

Table 3
Antihypertensive Use.

	Baseline	Longitudinal Analysis	
		Newly Added	Exposure ≥ 1 Year
n	610	381	381
ACEi or ARB	70 % (424)	29 % (112)	80 % (307)
ACE inhibitor	45 % (277)	14 % (55)	44 % (170)
ARB	28 % (168)	20 % (78)	41 % (158)
Diuretics	61 % (371)	19 % (73)	68 % (265)
Thiazide Diuretic	56 % (340)	18 % (70)	62 % (237)
K+ Sparing Diuretic	10 % (63)	13 % (49)	16 % (63)
Loop Diuretic	4 % (22)	5 % (21)	7 % (26)
Calcium Channel Blocker	40 % (246)	35 % (136)	58 % (224)
Dihydropyridine	34 % (208)	34 % (130)	53 % (204)
Non-Dihydropyridine	6 % (39)	3 % (13)	6 % (24)
Beta Blocker	35 % (215)	12 % (48)	37 % (143)
Alpha-1 Blocker	3 % (20)	8 % (32)	6 % (22)
Alpha-2 Agonist	2 % (12)	3 % (10)	2 % (8)
Hydralazine	1 % (6)	8 % (30)	4 % (15)
Nitrate	<1% (1)	<1% (2)	<1% (3)
Number of Anihypertensive Classes			
0	2 % (11)	30 % (116)	2 % (6)
1	22 % (137)	34 % (134)	14 % (54)
2	38 % (232)	23 % (90)	29 % (111)
3	28 % (175)	9 % (34)	30 % (115)
4	8 % (51)	2 % (9)	19 % (73)
5	< 1 % (4)	<1% (2)	6 % (22)
6+	0	0	1 % (4)

ACEi = angiotensin converting enzyme inhibitor. ARB = angiotensin receptor blocker.

Table 4
Regression Models for Longitudinal Perivascular Space Changes.

Model 1: Effect of Treatment on PVS Volume Fraction (n = 381)			
Fixed Effects Predictors:	coefficient	95 % CI	p-value
Timepoint	0.0017	−0.018 to 0.022	0.87
Intensive Treatment	−0.0021	−0.059 to 0.055	0.94
Interaction:			
Intensive Treatment × Time	−0.029	−0.055 to −0.0029	0.029
Adjusted for: age, sex, race, CVD, CKD, baseline SBP, MRI site, logWMH			
Model 2: Adjusted for Change in WMH and Total Brain Volumes (n = 381)			
Fixed Effects Predictors:	coefficient	95 % CI	p-value
Timepoint	0.027	0.0011 to 0.054	0.041
Intensive Treatment	0.0018	−0.054 to 0.058	0.95
Interaction:			
Intensive Treatment × Time	−0.026	−0.052 to −0.00040	0.047
Adjusted for: age, sex, race, CVD, CKD, baseline SBP, MRI site, WMH volume, change in WMH volume, TBV, and change in TBV			
Model 3: Effect of Antihypertensive Class (n = 381)			
Fixed Effects Predictors:	coefficient	95 % CI	p-value
Timepoint	0.020	−0.060 to 0.017	0.27
Interactions:			
ACEi / ARB × Time	0.020	−0.017 to 0.057	0.29
Beta Blockers × Time	−0.0053	−0.038 to 0.027	0.75
CCBs × Time	−0.038	−0.071 to −0.0048	0.025
Diuretics × Time	−0.021	−0.054 to 0.012	0.20
Adjusted for: age, sex, race, CVD, CKD, baseline SBP, treatment group, achieved SBP, MRI site, logWMH, TBV, and main effects for exposures to ACEi/ARB, Beta blockers, CCB, and diuretics			

PVS: perivascular spaces. CI: confidence intervals. CVD: cardiovascular disease. CKD: chronic kidney disease. SBP: systolic blood pressure. WMH: white matter hyperintensities. TBV: total brain volume. ACEi: ace inhibitors. ARB: angiotensin receptor blockers. CCBs: calcium channel blockers.

4. Discussion

PVS volume fraction reduced by 0.029 percentage points with intensive treatment to goal SBP < 120 mm Hg relative to standard treatment to goal SBP < 140 mm Hg, with an absolute reduction of −0.027 percentage points (−0.20 cm³) from baseline. When compared to the baseline association with age (0.004 percentage points larger per year older), the reduction in PVS volume fraction from baseline equated to an approximately 7-year reversal in age-related PVS enlargement (over median 3.9 years). Interestingly, even the standard treatment group showed a nonsignificant reduction of −0.0017 percentage points (−0.075 cm³) from baseline, which was still an attenuation of the effect of age on baseline PVS volume fraction. The reduction in PVS volume fraction was also associated with exposure to CCBs, but not the use of other antihypertensive classes, suggesting potential mechanisms for PVS changes. The implications of these findings are that intensive treatment is associated with PVS morphological changes, namely a partial reversal of the PVS enlargement seen with aging, hypertension, and increased vascular risk. It remains to be seen whether these SBP-related PVS alterations reflect improved glymphatic function and brain health or are merely an epiphenomenon of intensive SBP treatment.

The primary result of the SPRINT MRI substudy was that intensive treatment was associated with slower progression of WMH (Nasrallah et al., 2019). Our results demonstrated a partial reversal of PVS enlargement, suggesting that PVS may be more dynamic than other markers of CSVD. While some reversal of WMH has been shown (Wardlaw et al., 2017; van Leijsen et al., 2019), WMH are thought to reflect white matter injury through multiple proposed mechanisms that are largely irreversible. The primary SPRINT MRI publication also reported that intensive SBP treatment reduced TBV by 30.6 cm³ (−2.7 %) compared to 26.9 cm³ (−2.4 %) in the standard treatment group. PVS volumes did not account for this magnitude of change, being only 5.3 cm³ on average, and longitudinal PVS changes were much smaller (−0.20 cm³ vs −0.076 cm³). On the other hand, visible PVS may reflect

only a small fraction of subvoxel-sized PVS and other extracellular fluid spaces regulated via the glymphatic system. Conversely, total brain volume changes did not appear to completely account for the PVS change, since we used PVS volume fraction, a PVS density measure that accounted for changes to the underlying tissue. Furthermore, in a subsequent model we also adjusted for longitudinal change in TBV.

While we detected reversal of PVS enlargement seen with aging and CSVD, there is little evidence from human studies that PVS size directly relates to glymphatic function. One potential explanation for our findings could be that overall volume status was reduced in the intensive SBP treatment group, and that fluid shifts preferentially affected PVS. However, diuretic exposure was not associated with PVS volume reduction after adjusting for TBV. On the other hand, CCB exposure was associated with PVS volume reduction. CCBs, particularly dihydropyridines, exert antihypertensive effects primarily through arterial vasodilation, thereby increasing vascular compliance of the cerebral arteries. Improved cerebrovascular compliance may have reduced PVS size by facilitating bulk flow in the PVS and interstitial fluid through greater amplitude vasomotor oscillations. Prior SPRINT results in a different subsample found that the progression of aortic stiffness was attenuated in the intensive SBP treatment group (Upadhyaya et al., 2021), so it is possible that intensive treatment also improves cerebrovascular stiffness. However, there were multiple potential confounders in interpreting the relative effects of antihypertensive classes since medication exposure was not randomized. It is difficult to disentangle medication class effects from participants' comorbidities and prescriber preferences that would bias antihypertensive exposure. For example, while thiazide diuretics were the encouraged first-line agent, CCBs were the most common new antihypertensive added during the study. Furthermore, ACEis or ARBs were used by 80 % of participants, reducing the ability to detect a class effect. Finally, synergistic effects of antihypertensive combinations were not accounted for in our model.

The baseline associations between enlarged PVS and older age have been previously reported in studies using both visual PVS rating scales (Zhu et al., 2010; Heier et al., 1989) and PVS quantification (Kim et al., 2023). Some have suggested that enlarged PVS merely reflect local atrophy (Barkhof, 2004; Huang et al., 2021). However, in this study, we find that enlarged PVS volume fraction was positively associated brain parenchymal fraction, or less atrophy, although the regression coefficient was small. This finding is counterintuitive, but the positive association suggests that PVS enlargement reflects more than just brain atrophy. While we quantified PVS as a volume fraction reflecting PVS density within the tissue studied, prior studies also found increased PVS visibility was associated with larger intracranial volume (Huang et al., 2021).

Larger PVS volume fraction was also counterintuitively associated with a lower burden of WMH. This would seem to contradict multiple prior studies demonstrating increased PVS visibility in the setting of SVD and higher WMH burden (Rouhl et al., 2008; Potter et al., 2015). However, in this volumetric assessment, the PVS segmentation method restricted any overlap with WMH. So, a larger burden of WMH resulted in less white matter space to quantify PVS. In this older population with elevated cardiovascular risk, more severe WMH burden was common. While PVS run through WMH, and WMH are sometimes seen to develop around PVS, the overlap is difficult to distinguish on T2, so voxels containing WMH were excluded from PVS segmentations. To adjust for this discrepancy, we included logWMH as a covariate throughout all analyses. However, since WMH growth was attenuated in the intensive treatment group in the initial SPRINT MRI study, the inverse relationship between WMH and PVS volume fraction might have reduced the effect size of intensive treatment on PVS volume reduction. Given that the physiologic relationship between enlarging PVS and WMH remains unclear, a voxel-wise, longitudinal analysis co-localizing PVS and new WMH growth could provide further insight on the role of visible PVS in CSVD progression.

There are several limitations to this study. Of participants with

baseline MRI, 31 % did not have follow-up MRI, thus introducing potential retention bias. While the attrition was partially affected by early termination of the intervention (Nasrallah et al., 2019), loss to follow-up may have selected for healthier and more compliant participants. Furthermore, due to the small size of PVS, quantification is limited by motion and T2 image quality, and 9 % of scans were excluded due to insufficient image quality. This loss was compounded for the longitudinal analysis, with 16 % of participants excluded due to insufficient baseline or follow-up scans. While all images and segmentations were reviewed for quality and visually poor segmentations were excluded, there may have been a persistent effect of image quality on the volumetric segmentation of PVS in the remaining datasets. For the automatic PVS segmentation, a random subset of 120 scans were visually rated to determine the optimal threshold for the dataset, without individualizing for differences in MRI sites or local populations. While we adjusted for MRI site in all models, individualized thresholds could provide closer anatomical segmentation of PVS. However, MRI site sequences were coordinated using shared phantoms, and each participant had both scans performed at the same site. Furthermore, in determining the optimal Frangi threshold, the relationship between PVS volume fraction and visual ratings was stable over a wide range of thresholds, suggesting that small differences in thresholding would make little difference to the results.

5. Conclusions

Enlarged perivascular spaces are a dynamic marker of CSVD, and intensive SBP treatment is associated with partial reversal of the PVS enlargement seen with aging and vascular risk factors. While SBP lowering is associated with PVS remodeling, we also found an additional effect of exposure to calcium channel blockers, suggesting that improved vascular compliance may also relate to reduction of PVS volumes. While it remains to be seen whether these structural changes reflect improved glymphatic function, our findings implicate a potential mechanism by which intensive SBP treatment may improve brain health.

Funding

This analysis was funded by the NINDS Intramural Research Program. SPRINT was funded by NIH (NHLBI, NIDDK, NIA, and NINDS) under contracts HHSN268200900040C, HHSN268200900046C, HHSN268200900047C, HHSN268200900048C, and HHSN268200900049C and interagency agreement A-HL-13-002-001. It was also supported in part through the Department of Veterans Affairs. Azilsartan and chlorthalidone (combination) were provided by Takeda Pharmaceuticals.

Additional support was provided by National Center for Advancing Translational Sciences awards: UL1TR000439 (Case Western Reserve); UL1RR025755 (Ohio State); UL1RR024134 and UL1TR000003 (University of Pennsylvania); UL1RR025771 (Boston University); UL1TR000093 (Stanford); UL1RR025752, UL1TR000073, and UL1TR001064 (Tufts); UL1TR000050 (University of Illinois); UL1TR000005 (University of Pittsburgh); U54TR000017-06 (University of Texas Southwestern); UL1TR000105-05 (University of Utah); UL1TR000445 (Vanderbilt); UL1TR000075 (George Washington University); UL1TR000002 (University of California, Davis); UL1TR000064 (University of Florida); and UL1TR000433 (University of Michigan); and by National Institute of General Medical Sciences, Centers of Biomedical Research Excellence award NIGMSP30GM103337 (Tulane).

Disclosures

KCK: None. IMN: None. RNB: None. DMR: None. CBW: Honoraria from [uptodate.com](https://www.uptodate.com) for articles on vascular dementia. This article was not reviewed by the SPRINT Publications and Presentations Committee.

CRedit authorship contribution statement

Kyle C. Kern: Conceptualization, Formal analysis, Investigation, Methodology, Writing – original draft, Writing – review & editing. **Ilya M. Nasrallah:** Data curation, Investigation, Resources, Writing – review & editing. **Robert Nick Bryan:** Data curation, Investigation, Writing – review & editing. **David M. Reboussin:** Formal analysis, Methodology, Writing – review & editing. **Clinton B. Wright:** Conceptualization, Formal analysis, Investigation, Methodology, Resources, Writing – review & editing, Supervision.

Declaration of Competing Interest

The authors declare the following financial interests/personal relationships which may be considered as potential competing interests: Clinton B. Wright reports a relationship with Wolters Kluwer UpToDate that includes: consulting or advisory.].

Data availability

Data will be made available upon request. The SPRINT Trial data is available through NHLBI BioLINCC Repository (biolincc.nhlbi.nih.gov).

Acknowledgements

This work used the computational resources of the NIH HPC Biowulf cluster: hpc.nih.gov.

Appendix A. Supplementary data

Supplementary data to this article can be found online at <https://doi.org/10.1016/j.nicl.2023.103513>.

References

- Ballerini, L., Lovreglio, R., Valdés Hernández, M.D.C., Ramirez, J., MacIntosh, B.J., Black, S.E., Wardlaw, J.M., 2018. Perivascular spaces segmentation in brain MRI using optimal 3D filtering. *Sci. Rep.* 8 (1), 2132.
- Barisano, G., Seppehrband, F., Collins, H.R., Jillings, S., Jeurissen, B., Taylor, J.A., Schoenmakers, C., De Laet, C., Rukavishnikov, I., Nosikova, I., Litvinova, L., Rumshiskaya, A., Annen, J., Sijbers, J., Laureys, S., Van Ombergen, A., Petrovichev, V., Sinitsyn, V., Pechenkova, E., Grishin, A., zu Eulenburg, P., Law, M., Sunaert, S., Parizel, P.M., Tomilovskaya, E., Roberts, D.R., Wuyts, F.L., 2022. The effect of prolonged spaceflight on cerebrospinal fluid and perivascular spaces of astronauts and cosmonauts. *PNAS* 119 (17) e2120439119.
- Barkhof, F., 2004. Enlarged virchow-robin spaces: Do they matter? *J. Neurol. Neurosurg. Psychiatry* 75 (11), 1516–1517.
- Cabeen, R.P., Laidlaw, D.H., Toga, A.W., 2018. Quantitative imaging toolkit: Software for interactive 3D visualization, data exploration, and computational analysis of neuroimaging datasets. *ISMRM-ESMRMB Abstr.* 12–14.
- Cerri, S., Puonti, O., Meier, D.S., Wuerfel, J., Mühlau, M., Siebner, H.R., Van Leemput, K., 2021. A contrast-adaptive method for simultaneous whole-brain and lesion segmentation in multiple sclerosis. *Neuroimage* 225, 117471.
- Donahue, E.K., Murdos, A., Jakowec, M.W., Sheikh-Bahaei, N., Toga, A.W., Petzinger, G. M., Seppehrband, F., 2021. Global and regional changes in perivascular space in idiopathic and familial parkinson's disease. *Mov. Disord.* 36 (5), 1126–1136.
- Heier, L.A., Bauer, C.J., Schwartz, L., Zimmerman, R.D., Morgello, S., Deck, M.D., 1989. Large virchow-robin spaces: MR-clinical correlation. *AJNR Am. J. Neuroradiol.* 10, 929–936.
- Huang, P., Zhu, Z., Zhang, R., Wu, X., Jiaerken, Y., Wang, S., Yu, W., Hong, H., Lian, C., Li, K., Zeng, Q., Luo, X., Xu, X., Yu, X., Yang, Y., Zhang, M., 2021. Factors associated with the dilation of perivascular space in healthy elderly subjects. *Front. Aging Neurosci.* 13, 624732.
- Huijts, M., Duits, A., Staals, J., Kroon, A., Leeuw, P., Oostenbrugge, R., 2014. Basal ganglia enlarged perivascular spaces are linked to cognitive function in patients with cerebral small vessel disease. *Curr. Neurovasc. Res.* 11, 136–141.
- Iliff, J.J., Wang, M., Liao, Y., Plogg, B.A., Peng, W., Gundersen, G.A., Benveniste, H., Vates, G.E., Deane, R., Goldman, S.A., et al., 2012. A paravascular pathway facilitates csf flow through the brain parenchyma and the clearance of interstitial solutes, including amyloid beta. *Sci. Transl. Med.* 4, 147Ra111.
- Kim, H.G., Shin, N.-Y., Nam, Y., Yun, E., Yoon, U., Lee, H.S., Ahn, K.J., 2023. MRI-visible dilated perivascular space in the brain by age: The human connectome project. *Radiology* 306 (3), 213254.
- Lynch, K.M., Seppehrband, F., Toga, A.W., Choupan, J., 2022. Brain perivascular space imaging across the human lifespan. *bioRxiv*; [pre-print].
- Mestre, H., Tithof, J., Du, T., Song, W., Peng, W., Sweeney, A.M., Olveda, G., Thomas, J. H., Nedergaard, M., Kelley, D.H., 2018. Flow of cerebrospinal fluid is driven by arterial pulsations and is reduced in hypertension. *Nat. Commun.* 9, 4878.
- Nasrallah, I.M., Pajewski, N.M., Auchus, A.P., Chelune, G., Cheung, A.K., Cleveland, M. L., Coker, L.H., Crowe, M.G., Cushman, W.C., Cutler, J.A., Davatzikos, C., Desiderio, L., Doshi, J., Erus, G., Fine, L.J., Gaussoin, S.A., Harris, D., Johnson, K.C., Kimmel, P.L., Kurella Tamura, M., Launer, L.J., Lerner, A.J., Lewis, C.E., Martindale-Adams, J., Moy, C.S., Nichols, L.O., Oparil, S., Ogrocki, P.K., Rahman, M., Rapp, S.R., Reboussin, D.M., Rocco, M.V., Sachs, B.C., Sink, K.M., Still, C.H., Supiano, M.A., Snyder, J.K., Wadley, V.G., Walker, J., Weiner, D.E., Whelton, P.K., Wilson, V.M., Woolard, N., Wright, J.T., Wright, C.B., Williamson, J.D., Bryan, R.N., 2019. Association of intensive vs standard blood pressure control with cerebral white matter lesions. *J. Am. Med. Assoc.* 322 (6), 524.
- Potter, G.M., Chappell, F.M., Morris, Z., Wardlaw, J.M., 2015. Cerebral perivascular spaces visible on magnetic resonance imaging: Development of a qualitative rating scale and its observer reliability. *Cerebrovasc. Dis.* 39 (3–4), 224–231.
- Rennels, M.L., Gregory, T.F., Blaumanis, O.R., Fujimoto, K., Grady, P.A., 1985. Evidence for a 'paravascular' fluid circulation in the mammalian central nervous system, provided by the rapid distribution of tracer protein throughout the brain from the subarachnoid space. *Brain Res.* 326 (1), 47–63.
- Rouhl, R.P.W., van Oostenbrugge, R.J., Knottnerus, I.L.H., Staals, J.E.A., Lodder, J., 2008. Virchow-robin spaces relate to cerebral small vessel disease severity. *J. Neurol.* 255 (5), 692–696.
- Seppehrband, F., Barisano, G., Sheikh-Bahaei, N., Cabeen, R.P., Choupan, J., Law, M., Toga, A.W., 2019. Image processing approaches to enhance perivascular space visibility and quantification using MRI. *Sci. Rep.* 9, 12351.
- Seppehrband, F., Barisano, G., Sheikh-Bahaei, N., Choupan, J., Cabeen, R.P., Lynch, K.M., Crawford, M.S., Lan, H., Mack, W.J., Chui, H.C., Ringman, J.M., Toga, A.W., 2021. Volumetric distribution of perivascular space in relation to mild cognitive impairment. *Neurobiol. Aging* 99, 28–43.
- Smith, S.M., Jenkinson, M., Woolrich, M.W., Beckmann, C.F., Behrens, T.E.J., Johansen-Berg, H., Bannister, P.R., De Luca, M., Drobnjak, I., Flitney, D.E., Niaz, R.K., Saunders, J., Vickers, J., Zhang, Y., De Stefano, N., Brady, J.M., Matthews, P.M., 2004. Advances in functional and structural mr image analysis and implementation as fsl. *Neuroimage* 23 (Suppl. 1), S208–S219.
- SPRINT Research Group, Wright Jr., J.T., Williamson, J.D., Whelton, P.K., Snyder, J.K., Sink, K.M., Rocco, M.V., Reboussin, D.M., Rahman, M., Oparil, S., et al., 2015. A randomized trial of intensive versus standard blood-pressure control. *N. Engl. J. Med.* 373, 2103–2116.
- Upadhyay, B., Pajewski, N.M., Rocco, M.V., Hundley, W.G., Aurigemma, G., Hamilton, C. A., Bates, J.T., He, J., Chen, J., Chonchol, M., Glasser, S.P., Hung, A.M., Pisoni, R., Punzi, H., Supiano, M.A., Toto, R., Taylor, A., Kitzman, D.W., 2021. Effect of intensive blood pressure control on aortic stiffness in the SPRINT-HEART. *Hypertension* 77 (5), 1571–1580.
- van Leijsen, E.M.C., Bergkamp, M.I., van Uden, I.W.M., Cooijmans, S., Ghafoorian, M., van der Holst, H.M., Norris, D.G., Kessels, R.P.C., Platel, B., Tuladhar, A.M., de Leeuw, F.-E., 2019. Cognitive consequences of regression of cerebral small vessel disease. *Eur. Stroke J.* 4 (1), 85–89.
- van Veluw, S.J., Hou, S.S., Calvo-Rodriguez, M., Arbel-Ornath, M., Snyder, A.C., Frosch, M.P., Greenberg, S.M., Bacskaí, B.J., 2020. Vasomotion as a driving force for paravascular clearance in the awake mouse brain. *Neuron* 105 (3), 549–561.e5.
- Wardlaw, J.M., Chappell, F.M., Valdés Hernández, M.D.C., Makin, S.D.J., Staals, J., Shuler, K., Thrippleton, M.J., Armitage, P.A., Muñoz-Maniega, S., Heye, A.K., Sakka, E., Dennis, M.S., 2017. White matter hyperintensity reduction and outcomes after minor stroke. *Neurology* 89 (10), 1003–1010.
- Wardlaw, J.M., Benveniste, H., Nedergaard, M., Zlokovic, B.V., Mestre, H., Lee, H., Doubal, F.N., Brown, R., Ramirez, J., MacIntosh, B.J., Tannenbaum, A., Ballerini, L., Rungta, R.L., Boido, D., Sweeney, M., Montagne, A., Charkpak, S., Joutel, A., Smith, K.J., Black, S.E., 2020. Perivascular spaces in the brain: Anatomy, physiology and pathology. *Nat. Rev. Neuro.* 16 (3), 137–153.
- Williamson, J.D., Pajewski, N.M., Auchus, A.P., Bryan, R.N., Chelune, G., Cheung, A.K., Cleveland, M.L., Coker, L.H., Crowe, M.G., Cushman, W.C., Cutler, J.A., Davatzikos, C., Desiderio, L., Erus, G., Fine, L.J., Gaussoin, S.A., Harris, D., Hsieh, M.-K., Johnson, K.C., Kimmel, P.L., Tamura, M.K., Launer, L.J., Lerner, A.J., Lewis, C.E., Martindale-Adams, J., Moy, C.S., Nasrallah, I.M., Nichols, L.O., Oparil, S., Ogrocki, P.K., Rahman, M., Rapp, S.R., Reboussin, D.M., Rocco, M.V., Sachs, B.C., Sink, K.M., Still, C.H., Supiano, M.A., Snyder, J.K., Wadley, V.G., Walker, J., Weiner, D.E., Whelton, P.K., Wilson, V.M., Woolard, N., Wright, J.T., Wright, C.B., 2019. Effect of intensive vs standard blood pressure control on probable dementia: A randomized clinical trial. *JAMA – J. Am. Med. Assoc.* 321 (6), 553–561.
- Zhu, Y.-C., Dufouil, C., Soumaré, A., Mazoyer, B., Chabriat, H., Tzourio, C., 2010. High degree of dilated virchow-robin spaces on MRI is associated with increased risk of dementia. *J. Alzheimers Dis.* 22 (2), 663–672.